JOURNAL PRE-PROOF

This is an early version of the article, published prior to copyediting, typesetting, and editorial correction. The manuscript has been accepted for publication and is now available online to ensure early dissemination, author visibility, and citation tracking prior to the formal issue publication.

It has not undergone final language verification, formatting, or technical editing by the journal's editorial team. Content is subject to change in the final Version of Record.

To differentiate this version, it is marked as "PRE-PROOF PUBLICATION" and should be cited with the provided DOI. A visible watermark on each page indicates its preliminary status.

The final version will appear in a regular issue of *Engineering Transactions*, with final metadata, layout, and pagination.

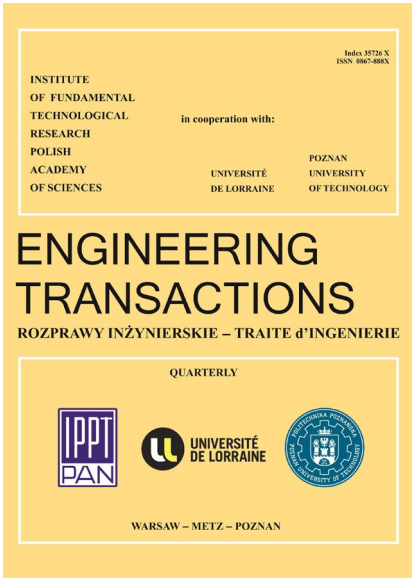

Title: Multi-Objective Optimization of Hobbing Process Parameters Based on Response Surface Method

Author(s): Yazhou Wang, Xiaohui Yin

DOI: https://doi.org/10.24423/engtrans.2025.3453

Journal: *Engineering Transactions*

ISSN: 0867-888X, e-ISSN: 2450-8071

Publication status: In press

Received: 2024-10-23

Revised: 2025-05-14

Accepted: 2025-06-08

Published pre-proof: 2025-12-12

Please cite this article as:

Wang Y., Yin X., Multi-Objective Optimization of Hobbing Process Parameters Based on Response Surface Method, *Engineering Transactions*, 2025, https://doi.org/10.24423/engtrans.2025.3453

Multi-Objective Optimization of Hobbing Process Parameters Based on Response Surface Method

Yazhou WANG*, Xiaohui YIN

School of Mechanical and Electrical Engineering
Lanzhou University of Technology, Lanzhou, China
*Corresponding Author e-mail: wangyzh@lut.edu.cn

In hobbing machining, gear geometric accuracy is an important factor affecting gear working performance, which is determined by the interaction of different process parameters. To improve the geometric accuracy of hobbing surface and obtain the minimum geometric error, this paper adopts the response surface method (RSM) to study the effects of various technological parameters on the geometric accuracy, and explores the influence law of various factors on the geometric accuracy through the response surface diagram. The mathematical models of total profile deviation, total helix deviation, cumulative total deviation of tooth spacing and radial runout were established based on response surface method, and the reliability of the models was tested by variance analysis. Non-dominated sorting whale optimization algorithm (NSWOA) was used to solve the mathematical model, and Pareto solution set was obtained. Entropy weight-TOPSIS method was used to determine the optimal scheme after NSWOA algorithm optimization. After optimization, the total deviation of tooth profile is reduced by 8.04 %, the total deviation of helix is reduced by 9.17 %, the cumulative total deviation of tooth spacing is reduced by 3.88 %, and the radial runout is reduced by 7.45 %, which proves that the optimized scheme can improve the gear accuracy after hobbing machining, and provides a reference for the reasonable selection of gear hobbing process parameters.

Keywords: hobbing machining; response surface method; multi-objective optimization; geometric accuracy.

1. Introduction

Gears are key components that affect the performance of machinery and equipment, and under economic and environmental constraints, industrial practices have been pursuing high-

precision gear manufacturing technology [1]. Hobbing technology is dominant in the field of gear manufacturing with its excellent processing efficiency and extensive process adaptability. Therefore, it is of great significance to study the hobbing accuracy to improve the efficiency of gear machining. Sun *et al*. [2] proposed a prediction model for geometric deviation of hobbing and an optimization model for hobbing process, which improved the machining accuracy of hobbing. Hu *et al*. [3] proposed an analysis method for the hobbing accuracy of flexible spline tooth profiles, which provides a valuable technical reference for error tracking and compensation in the process of hobbing. Wang *et al*. [4] considered energy consumption and gear geometrical deviations to optimize hobbing parameters. Matsuo *et al*. [5] described a hobbing simulation that was considered the first step in improving the accuracy of hobbing. The simulation aims to elucidate the effect of the positional relationship between the workpiece and the tool on the accuracy of the gear, including the pitch error of the workpiece and tooth runout. In order to improve the geometric accuracy of gear hobbing, many researchers have studied the process parameters. Zhou *et al*. [6] analyzed the basic principle of dry cutting technology and explored the law of the effect of changes in processing parameters on the cutting process. Dong *et al*. [7] constructed a three-dimensional finite element simulation model to simulate the complex motion between the hobbing tool and the gear workpiece, and conducted a coupled thermodynamic analysis of the tool and the workpiece during the chip removal process. Klockea *et al*. [8] designed a continuous gear hobbing simulation method, which can numerically reproduce the cutting process in complex processing environments and predict the geometric profile and surface features of the workpiece.

Process parameter optimization is the key technology to improve the machining performance of hobbing, the core of which is to realize the collaborative improvement of machining efficiency and machining precision through parameter optimization. Multi-objective optimization [9] adopts a global optimization strategy, establishes a comprehensive evaluation system including key indicators such as processing cost, processing efficiency and processing accuracy, and uses impact analysis method to determine the optimal combination of process parameters, so as to achieve the overall optimization of processing performance. Kane *et al.*

[10] adopted a mathematical modeling method to build a univariate optimization model aiming at minimizing the processing cost. In this model, hob speed and feed rate were taken as key decision variables, and the optimal process parameter combination was obtained by solving the objective function. Li *et al.* [11] proposed a multi-objective optimization method of process parameters considering the minimum heat accumulation of dry gear hobbing machine spindle, which effectively reduced the average temperature of the machine tool spindle. Santanna *et al.* [12] took the tool vibration characteristics as the optimization objective, and revealed the internal correlation between the hobbing process parameters and the tool vibration through experimental research methods. On the premise of maintaining the stability of the tool system, the optimization method could increase the machining efficiency by more than 18%.

The application of intelligent algorithms to process parameter optimization is one of the current research hotspots in the fields of engineering and manufacturing. Its core lies in efficiently finding the optimal process combination through data-driven and intelligent search strategies to enhance production efficiency, reduce costs or improve product quality [13]. Sun *et al.* [2] took the minimum gear geometric error as the target, combined the improved particle swarm optimization algorithm and BP neural network to optimize the machining parameters. The optimized hobbing parameters improve the geometric accuracy of the gear. Wu *et al.* [14] constructed a multi-parameter collaborative optimization framework centered on processing efficiency and economy in response to the demand for improving the efficiency of gear hobbing process. They took the feed rate and cutting speed as key variables and conducted parameter tuning by integrating intelligent algorithms and data-driven prediction models. This method promotes energy conservation and consumption reduction in the production process while ensuring processing quality by integrating group optimization strategies and machine learning techniques.

Current research on hobbing process optimization mainly focuses on multi-objective collaborative optimization of energy consumption, time, quality and cost. With the development of Industry 4.0 and intelligent manufacturing, the optimization goal of gears, as a key basic component, has shifted from traditional efficiency and economic indicators to precise control

of geometric accuracy. The key geometric precision indexes such as total profile deviation, total helix deviation, cumulative total pitch deviation and radial runout directly affect the transmission performance of gear pairs. Therefore, modern hobbing process optimization needs to establish a geometric precision oriented model, which is regarded as the core optimization goal, and realize the collaborative optimization of each key index.

2. Methods

2.1. Test conditions

The KE180 hobbing machine of Kashifuji company is used as the hobbing processing equipment, the on-site hobbing equipment and processing area are shown in Fig. 1, the gear model and the processed gear are shown in Fig. 2, and the basic parameters of hob and gear are shown in Table 1 [15]. The material of the gear is 20CrMnTi, which has the characteristics of high hardness, wear resistance and good toughness, and is widely used in gear manufacturing, and its mechanical properties are shown in Table 2.

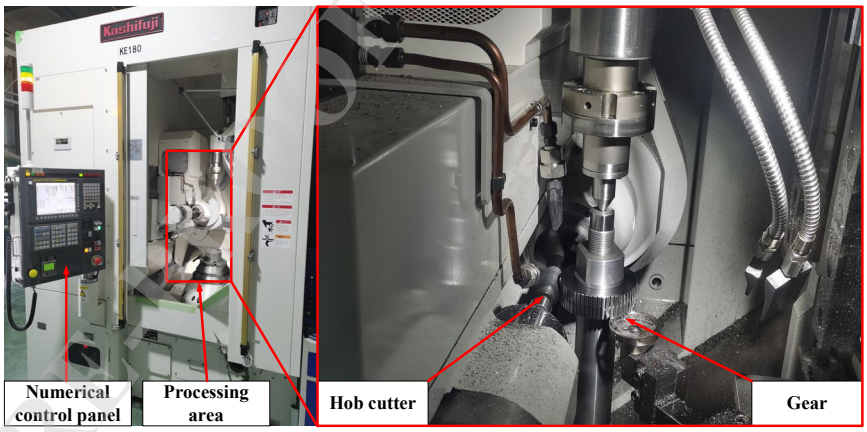

Fig. 1. Hobbing equipment and processing area.

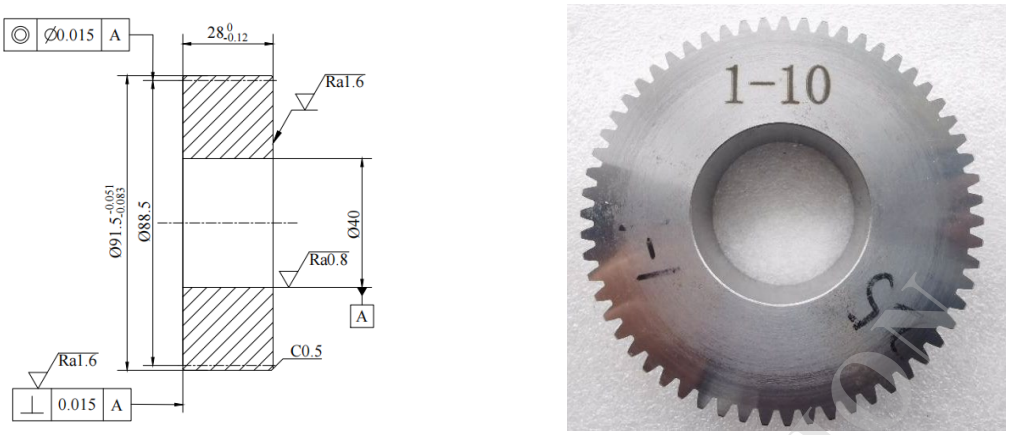

a) b)

Fig. 2. Gear model (a) and machined gears (b).

Table 1. Main parameters of hobs and gears.

Hob parameters		Gear parameters	
Normal modulus [mm]	1.5	Modulus [mm]	1.5
Number of heads	1	Number of teeth	59
Normal pressure angle [°]	20	Pressure angle [°]	20
Spiral rising angle	3°3′	Tooth width [mm]	28

Table 2. 20CrMnTi mechanical properties.

Tensile strength [MPa]	Yield strength [MPa]	Elongation [%]	Section shrinkage [%]
≥1080	≥835	≥10	≥45

2.2. Test scheme

During the test process, only the machining parameters (hob speed V, feed rate f, and back engagement D) are changed to explore the influence law of hobbing machining technology on geometric accuracy. The basic deviation of gear tooth surface (total deviation of tooth profile F_α, total deviation of helix F_β, cumulative total deviation of tooth spacing F_p, and radial runout F_r) was selected as the evaluation index for geometric accuracy [16, 17]. The difference in the back engagement represents the difference in the times of cuts. To facilitate operation and

analysis in the software, the back engagement D is expressed by the times of cuts D_t. The test scheme of three factors and three levels was obtained, and the test factors and levels were shown in Table 3. Box-Benhnken experimental Design method (BBD) was used to design the response surface test [18], and Design-Expert software was used to conduct the test design. A total of 17 tests were conducted, and the test scheme was shown in Table 4.

Table 3. Test factors and level.

Level	Hob speed [r/min]	Feed rate [mm/min]	Back engagement [mm]
1	450	2	0.84375 (4 times)
2	600	2.75	1.125 (3 times)
3	750	3.5	1.6875 (2 times)

Table 4. Response surface test scheme.

No.	Hob speed [r/min]	Feed rate [mm/min]	Back engagement [mm]	No.	Hob speed [r/min]	Feed rate [mm/min]	Back engagement [mm]
1	600	2.75	1.125	10	600	2.75	1.125
2	750	2	1.125	11	600	2	0.84375
3	600	3.5	0.84375	12	600	3.5	1.6875
4	600	2.75	1.125	13	450	2.75	1.6875
5	750	3.5	1.125	14	600	2.75	1.125
6	600	2	1.6875	15	450	2.75	0.84375
7	750	2.75	0.84375	16	600	2.75	1.125
8	750	2.75	1.6875	17	450	2	1.125
9	450	3.5	1.125				

2.3. Geometric accuracy measurements

The Japanese OSAKA Precision CLP-35SF automatic gear measuring instrument is used to measure the gear geometric error, and the on-site measurement equipment and measurement area are shown in Fig. 3 [19]. The testing specification is implemented according to ISO1328-

1:2013, and the detection precision level is determined according to ISO1328-1:2013. As shown in Fig. 4, the total deviation of tooth profile and the total deviation of helix at a total of 8 measurement positions were selected from the left and right tooth surfaces of four gear teeth numbered 01, 16, 31, and 46, and the corresponding higher values of total deviation of tooth profile and total deviation of helix were selected for analysis [16]. The cumulative total deviation of tooth spacing and the radial runout were measured on the left and right flanks of the 59 teeth of each gear, and the average value of cumulative total deviation of tooth spacing and radial runout were selected for analysis [20].

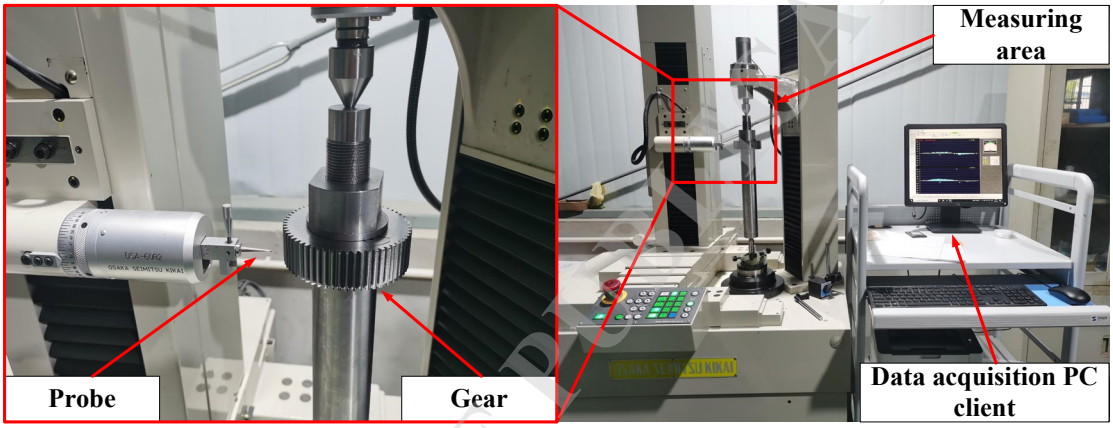

Fig. 3. Measurement process of the CLP-35SF fully automatic gear measuring instrument.

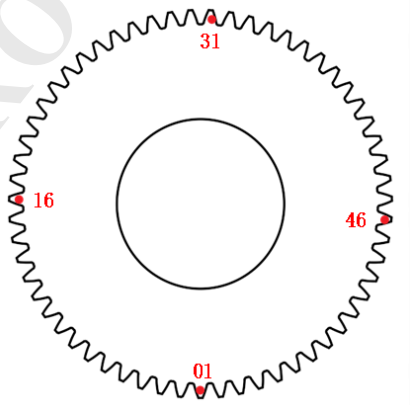

Fig. 4. Schematic diagram of the location of the measurement point of the total deviation of tooth profile and the total deviation of helix.

2.4. Optimization based on NSWOA

Different from the unique optimality of single objective function, the multi-objective

function model should consider the mutual restriction and influence of multiple objective functions in solving. In the process of gear hobbing, the guarantee of machining geometric accuracy is the primary condition to meet the performance requirements. The total profile deviation, total helix deviation, cumulative total pitch deviation and radial runout are the key optimization objectives, and their mutual restriction relationship and synergistic influence should be comprehensively considered. Therefore, multi-objective optimization was carried out with hobbing process parameters (hob speed, feed rate, back engagement) as optimization variables, total profile deviation, total helix deviation, cumulative total deviation of tooth spacing and radial runout as optimization objectives.

2.4.1. Optimization objectives and constraints

The NSWOA algorithm was used to optimize the total deviation of tooth profile, total deviation of helix, cumulative total deviation of tooth spacing and radial runout. The difference in the back engagement represents the difference in the times of cuts. In order to facilitate calculation, back engagement D is expressed by the times of cutting D_t. Therefore, the NSWOA algorithm is used to optimize and combine V, f, and D_t. Based on the set range of process parameters, the interval distribution of measurement data, and the minimum size characteristics of the optimization objective, constraint conditions are established. The optimization objective and constraint conditions are as follows:

$$
\begin{cases}
\min F_\alpha(V,f,D_t), \\
\min F_\beta(V,f,D_t), \\
\min F_p(V,f,D_t), \\
\min F_r(V,f,D_t), \\
9\ \mu\text{m} \le F_\alpha(V,f,D_t) \le 12.8\ \mu\text{m}, \\
22\ \mu\text{m} \le F_\beta(V,f,D_t) \le 47.9\ \mu\text{m}, \\
10.5\ \mu\text{m} \le F_p(V,f,D_t) \le 52.8\ \mu\text{m}, \\
13.2\ \mu\text{m} \le F_r(V,f,D_t) \le 58.8\ \mu\text{m}, \\
450\ \text{r/min} \le V \le 750\ \text{r/min}, \\
2\ \text{mm/min} \le f \le 3.5\ \text{mm/min}, \\
2\ \text{times} \le D_t \le 4\ \text{times},
\end{cases}
\tag{2.1}
$$

where V, f, D_t represent hob speed, feed rate, and cutting times, respectively.

The penalty function method is adopted to handle the constraint conditions, and the form

of the penalty function is as follows:

$$\Phi_k(x) = f_k(x) + P(x), \quad k = 1, 2, \ldots, m. \tag{2.2}$$

where $f_k(x)$ is the original objective function and $P(x)$ is the penalty term, which is used to punish the solutions that violate the constraints.

2.4.2. Solving procedure

The solution procedure of the NSWOA algorithm [21, 22] is as follows: In the first stage, the set of whales and prey randomly generated by the whale population and their position vectors are initialized, and then the fitness of each whale position is calculated according to the objective function. In the second stage, the non-dominated solution in the initial population is determined and saved in the Pareto archive, the crowding distance of each Pareto solution is calculated, the position vector is selected based on the crowding distance value, and then the position vector is calculated and the position of the whale is updated using equations:

$$\vec{X}(t+1) = \overrightarrow{D'} * e^{bt} * \cos(2\pi l) + \vec{X} * (t), \tag{2.3}$$

$$\overrightarrow{D'} = \left|\vec{X} * (t) - X(t)\right|, \tag{2.4}$$

$$\vec{X}(t+1) = \begin{cases} \vec{X} * (t) - \vec{X}\vec{X} \text{ if } p < 0.5, \\ \overrightarrow{D'} \cdot e^{bt} \cdot \cos(2\pi l) + \vec{X} * (t) \text{ if } p > 0.5, \end{cases} \tag{2.5}$$

$$\vec{D} = \left|\vec{C} \cdot \overrightarrow{X_{rand}} - \vec{X}\right|, \tag{2.6}$$

$$\vec{X}(t+1) = \overrightarrow{X_{rand}} - \vec{A} \cdot \vec{D}. \tag{2.7}$$

$$\mathbf{X}(t+1) = \mathbf{D}' * e^{bt} * \cos(2\pi l) + \mathbf{X}^*(t), \tag{2.3}$$

$$\mathbf{D}' = |\mathbf{X}^*(t) - \mathbf{X}(t)|, \tag{2.4}$$

where l is a random number [-1, 1], b is constant defines logarithmic shape, the asterisk represents simple multiplication, $\mathbf{D}'$ expresses the distance between i-th whale to the prey mean best solution so far.

Note, we assume that there is 50% probability that whale either follow the shrinking encircling or logarithmic path during optimization. Mathematically we modelled as follows:

$$\mathbf{X}(t+1) = \begin{cases} \mathbf{X}^*(t) - \mathbf{X} \cdot \mathbf{X} \text{ if } p < 0.5, \\ \mathbf{D}' * e^{bl} * \cos(2\pi l) + \mathbf{X}^*(t) \text{ if } p > 0.5, \end{cases} \tag{2.5}$$

where p expresses random number between [0, 1].

Vector $\mathbf{A}$ can be used for exploration to search for prey; vector $\mathbf{A}$ also takes the values greater than one or less than –1. Exploration follows two conditions:

$$\mathbf{D} = |\mathbf{C} * \mathbf{X}_{\text{rand}} - \mathbf{X}|, \tag{2.6}$$

$$\mathbf{X}(t+1) = \mathbf{X}_{\text{rand}} - \mathbf{A} \cdot \mathbf{D}\,. \tag{2.7}$$

Finally follows these conditions: $|\mathbf{A}| > 1$ enforces exploration to WOA algorithm to find out global optimum avoid local optima; $|\mathbf{A}| < 1$ for updating the position of current search agent / best solution is selected.

In the third stage, the fitness values of all update locations of whales are calculated, new non-dominated solutions in the population are determined and saved in Pareto files and any dominant solutions in Pareto files are eliminated. The crowding distance values of each Pareto solution are calculated, non-dominated sorting is performed according to the crowding distance mechanism, and global optimal solutions of rank 1 and rank 2 are selected. Output the optimal Pareto solution set.

2.4.3. Entropy weight – TOPSIS comprehensive evaluation

The entropy weight method is an objective weight determination method based on the principle of information theory, which reflects the importance of each indicator by quantifying the information entropy value of the indicators. The good and bad solution distance method (Technique for Order Preference by Similarity to Ideal Solution, TOPSIS) is a comprehensive evaluation method widely used in multi-objective decision analysis. This method realizes the scientific evaluation and ranking of multi-index and multi-scheme systems by calculating the relative proximity of each scheme to positive and negative ideal solutions. It is an effective method applicable to complex decision-making scenarios. The multi-criteria decision-making

method based on the entropy weight – TOPSIS method mainly includes the following implementation steps: In the initial stage, a standardized decision matrix needs to be constructed, and then the weight coefficients of each evaluation index are calculated using the entropy weight method. On this basis, the positive and negative ideal solutions of the scheme set are determined respectively, and the Euclidean distances between each scheme and the positive and negative ideal solutions are calculated. By establishing a comprehensive evaluation function, the comprehensive score values of each scheme are calculated, and they are ranked and selected based on the scores from high to low. Among them, the higher the score, the closer the scheme is to the positive ideal solution and the better the quality of the scheme is. This paper combines the entropy weight method with the TOPSIS method to screen out the optimal solution from the Pareto solution set optimized and generated by the NSWOA algorithm.

2.4.4. Multi-objective optimization process

The multi-objective optimization process of hobbing process parameters is as follows: the total deviation of tooth profile, total deviation of helix, cumulative total deviation of tooth spacing and radial runout are determined as optimization objectives; Hob speed, feed rate and cutting numble are determined as optimization variables, and their constraint conditions are determined. The regression models of total profile deviation, total helix deviation, cumulative total deviation of tooth spacing and radial runout based on the response surface test data were used as objective function models. The objective function model is solved by NSWOA algorithm. Pareto solution set of hobbing process parameters is obtained, and the optimal scheme optimized by NSWOA algorithm is determined by entropy weight method and TOPSIS method. The flow chart is shown in Fig. 5.

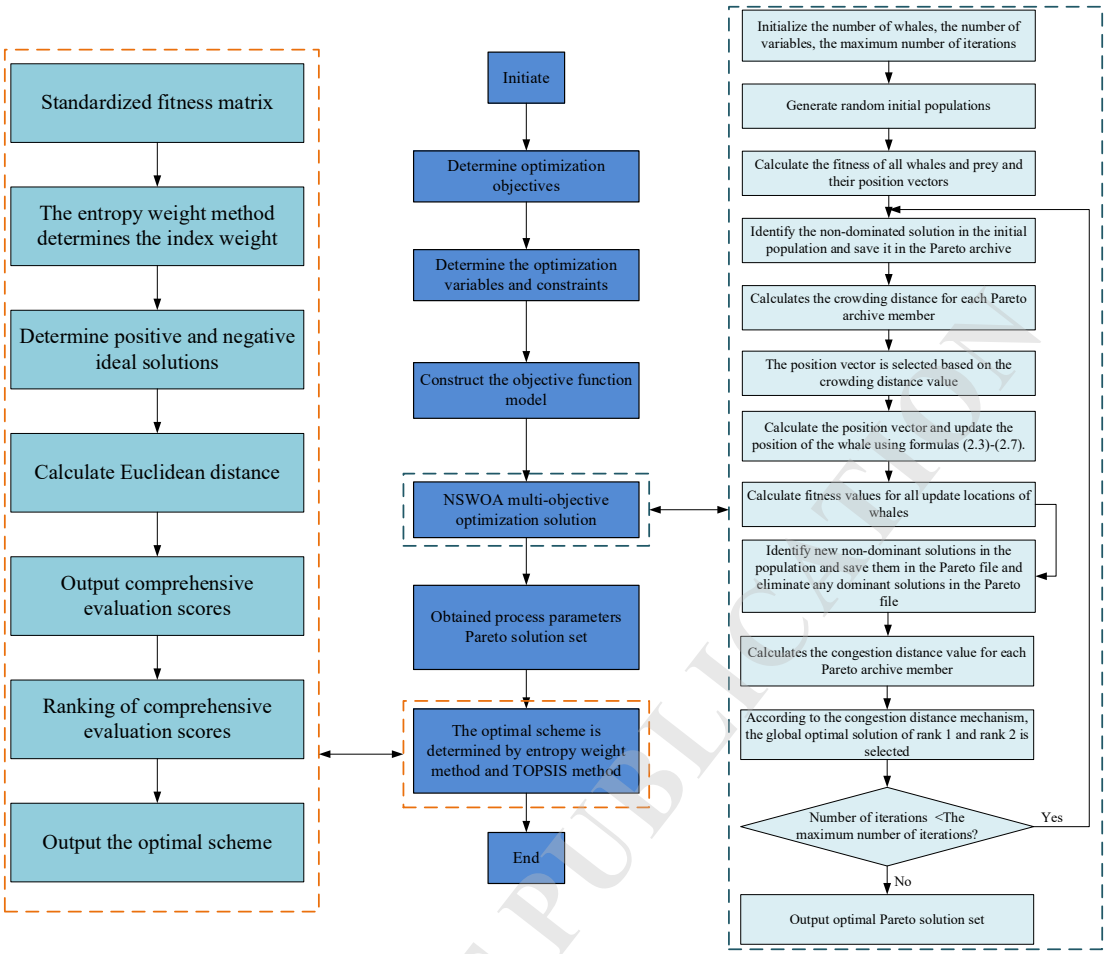

Fig. 5. Multi-objective optimization flow chart of gear hobbing process parameters.

3. Results and discussion

3.1. Establishment of mathematical model

The geometric accuracy measurement results of response surface test are shown in Table 5. In this study, stepwise regression analysis was adopted, and Design-Expert 13.0 software was used to model the total deviation of tooth profile, total deviation of helix, cumulative total deviation of tooth spacing and radial runout. The ternary quadratic regression model of hob speed, feed rate, back engagement and total deviation of tooth profile, total deviation of helix, cumulative total deviation of tooth spacing and radial runout is obtained. In order to facilitate operation and analysis in the software, the back engagement D is expressed by the times of cutting D_t . The mathematical model of tooth surface geometric accuracy established according to response surface method is as follows:

(3.1) $$F_{\alpha} = 11.90472 - 0.000672V - 4.67556f + 5.20250D_t + 0.008444Vf + 0.000167VD_t + 0.8fD_t - 0.000023V^2 - 0.537778f^2 - 1.17750{D_t}^2,$$

(3.2) $$F_{\beta} = 105.08944 - 0.307144V + 69.70222f - 51.335D_t - 0.005778Vf + 0.053VD_t - 6.8fD_t + 0.000125V^2 - 7.98222f^2 + 5.96{D_t}^2,$$

(3.3) $$F_P = 236.37333 + 0.21985V - 148.10667f - 58.05333D_t + 0.002Vf + 0.034167VD_t + 5.06667fD_t - 0.000245V^2 + 25.48f^2 + 3.0075{D_t}^2,$$

(3.4) $$F_r = 215.14611 + 0.1619V - 103.65444f - 69.37583D_t - 0.01Vf + 0.038833VD_t + 2.86667fD_t - 0.000192V^2 + 20.36444f^2 + 5.055{D_t}^2.$$

Table 5. Measurement results of geometric accuracy of response surface test.

No.	Total deviation of tooth profile [μm]	Total deviation of helix [μm]	Cumulative total deviation of tooth spacing [μm]	Radial runout [μm]
1	12	27.6	28.9	28.9
2	9.4	22	35.8	32.2
3	11.2	22.4	46.55	45.4
4	11	23.3	28.5	30.8
5	11.4	23	46.7	44.7
6	11	23.3	45.55	45
7	10	38.5	25.85	27.6
8	9	28.1	24.05	29.7
9	11	28.9	31.2	37.4
10	12.6	27	25.35	28.1

11	10.6	29.1	24.1	23
12	9.2	37	52.8	58.8
13	10.6	47.9	29.2	38.6
14	12.2	28.3	20.4	19.4
15	11.5	26.5	10.5	13.2
16	12.1	26.2	21.4	25.5
17	12.8	25.3	21.2	20.4

3.2. Model analysis

The regression analysis of these four mathematical models shows that the correlation coefficients R^2 of the total profile deviation, total helix deviation, cumulative total pitch deviation and radial runout regression models are all greater than 0.9. (According to the definition of the coefficient of correlation R^2, its value ranges from [0, 1]. When R^2 approaches 1, it indicates that the prediction accuracy of the regression model is higher, the error has less influence on the result, and the fitting effect of the model is more ideal.) This indicates that the total profile deviation, the total helix deviation, the cumulative total pitch deviation and the radial runout regression model have sufficient prediction accuracy.

Table 6 shows the ANOVA results of the total tooth profile deviation regression model. Where the *F*-value is the key statistic of ANOVA, which is used to evaluate the significant difference of variance between the factors. In general, when $F \geq 4$, it indicates that the variation of design parameters has a significant impact on model performance. The *P*-value is used to measure the statistical significance of the *F*-value. If $P \leq 0.05$, it indicates that the factor has a significant impact on the response variable. In addition, when the *P*-value of the misfit term is greater than 0.05, it indicates that the proportion of abnormal error in the regression equation is low, and the fitting effect between the model and the actual data is good. The *F*-value of the model item is 9.03 and the *P*-value is 0.0042, which reflects the high significance of the

regression model. At the same time, the *F*-value of the missing fitting item is 0.2438 and the *P*-value is 0.8621, which further indicates that the influence of the lack of fitting is not significant compared with the pure error, and the model has strong explanatory ability and reliability. In this case, V, D_t, Vf, fD_t, and D_t^2 are important factors. The correlation coefficient R^2 of the model is 0.9207, indicating that the model has a high degree of fit.

Table 6. Analysis of variance for regression fitting of total deviation of tooth profile.

Source	Sum of squares	*Df*	Mean square	*F*-value	*P*-value	Significance
Model	19.33	9	2.15	9.03	0.0042	significant
V	4.65	1	4.65	19.55	0.0031	
f	0.1250	1	0.1250	0.5254	0.4921	
D_t	1.53	1	1.53	6.44	0.0388	
Vf	3.61	1	3.61	15.17	0.0059	
VD_t	0.0025	1	0.0025	0.0105	0.9212	
fD_t	1.44	1	1.44	6.05	0.0435	
V^2	1.17	1	1.17	4.92	0.0620	
f^2	0.3853	1	0.3853	1.62	0.2438	
D_t^2	5.84	1	5.84	24.54	0.0016	
Residual	1.67	7	0.2379			
Lack of fit	0.2575	3	0.0858	0.2438	0.8621	not significant
Pure error	1.41	4	0.3520			
Cor total	21.00	16				
$R^2 = 0.9207$						

According to the ANOVA results of the total helix deviation regression model in Table 7, the *F*-value of the model item is 33.7, and the *P*-value is less than 0.0001, indicating that the regression model has extremely high significance. In addition, the *F*-value of the missing fitting item is 0.1393 and the *P*-value is 0.9314, indicating that the influence of the lack of fitting is

not significant compared with the pure error, and the model can fully explain the change law of the data, with good applicability and reliability. In this case, V, f, D_t, VD_t, fD_t, V^2, f^2, and D_t^2 are significant factors. The correlation coefficient R^2 of the model is 0.9774, and the fit degree is very high.

Table 7. Analysis of variance for regression fitting of helix total deviation.

Source	Sum of squares	*Df*	Mean Square	*F*-value	*P*-value	Significance
Model	719.11	9	79.90	33.70	< 0.0001	significant
V	36.12	1	36.12	15.24	0.0059	
f	16.82	1	16.82	7.09	0.0323	
D_t	49.00	1	49.00	20.67	0.0026	
Vf	1.69	1	1.69	0.7127	0.4264	
VD_t,	252.81	1	252.81	106.62	< 0.0001	
fD	104.04	1	104.04	43.88	0.0003	
V^2	33.25	1	33.25	14.02	0.0072	
f^2	84.88	1	84.88	35.80	0.0006	
D_t^2	149.56	1	149.56	63.08	< 0.0001	
Residual	16.60	7	2.37			
Lack of fit	1.57	3	0.5233	0.1393	0.9314	not significant
Pure error	15.03	4	3.76			
Cor total	735.71	16				
$R^2 = 0.9774$						

Table 8 shows the ANOVA results of the regression model of cumulative total deviation of tooth spacing. The *F*-value of the model term is 11.18 and the *P*-value is 0.0022, indicating that the regression equation is highly significant. At the same time, the *F*-value of the missing fitting item is 1.59 and the *P*-value is 0.3235, indicating that the influence of the lack of fitting is not significant compared with the pure error, and the model can effectively explain the trend

of data change, with strong reliability and applicability. In this case, V, f, D_t, V^2, and f^2 are significant factors. The correlation coefficient of the model is 0.9350, and the fit degree is high.

Table 8. Analysis of variance for regression fitting of cumulative total deviation of tooth spacing.

Source	Sum of squares	*Df*	Mean square	F-value	P-value	Significance
Model	1947.25	9	216.36	11.18	0.0022	significant
V	203.01	1	203.01	10.49	0.0143	
f	320.04	1	320.04	16.54	0.0048	
D_t	248.64	1	248.64	12.85	0.0089	
Vf	0.2025	1	0.2025	0.0105	0.9214	
VD_t,	105.06	1	105.06	5.43	0.0526	
fD_t,	57.76	1	57.76	2.99	0.1276	
V^2	128.18	1	128.18	6.63	0.0368	
f^2	864.93	1	864.93	44.71	0.0003	
D_t^2	38.08	1	38.08	1.97	0.2034	
Residual	135.42	7	19.35			
Lack of fit	73.76	3	24.59	1.59	0.3235	not significant
Pure error	61.66	4	15.42			
Cor total	2082.67	16				
$R^2 = 0.9350$						

According to the ANOVA results of the radial runout regression model in Table 9, the *F*-value of the model item is 13.6 and the *P*-value is 0.0012, indicating that the regression equation has extremely high significance. In addition, the *F*-value of the missing fitting item is 0.6228 and the P-value is 0.6367, indicating that the influence of the lack of fitting is not significant compared with the pure error, and the model can fully explain the change law of the data, with good applicability and reliability. In this case, f, D_t, VD_t, f^2, and D_t^2 are significant factors. The correlation coefficient of the model is 0.9459, and the fit degree is high.

Table 9. Analysis of variance for radial runout regression fitting.

Source	Sum of squares	*Df*	Mean square	*F*-value	*P*-value	Significance
Model	2005.73	9	222.86	13.6	0.0012	significant
V	75.65	1	75.65	4.61	0.0688	
f	539.56	1	539.56	32.92	0.0007	
D_t	494.55	1	494.55	30.17	0.0009	
Vf	5.06	1	5.06	0.3088	0.5957	
VD_t	135.72	1	135.72	8.28	0.0237	
fD_t	18.49	1	18.49	1.13	0.3235	
V^2	78.58	1	78.58	4.79	0.0647	
$f2$	552.49	1	552.49	33.7	0.0007	
D_t^2	107.59	1	107.59	6.56	0.0374	
Residual	114.74	7	16.39			
Lack of fit	36.53	3	12.18	0.6228	0.6367	Not significant
Pure error	78.21	4	19.55			
Cor total	2120.47	16				
$R^2 = 0.9459$						

3.3. Response surface diagram analysis

The response surface diagram can more intuitively understand the interaction effect between factors, the change trend of response variables, and the direction and intensity of interaction. Figure 6 is the response surface diagram of the total tooth profile deviation, in which Fig. 6a is the response surface diagram of the influence of hob speed and feed rate on the total tooth profile deviation. When the feed rate is constant, the total tooth profile deviation decreases with the increase of hob speed. When the hob speed is constant, the total deviation of tooth profile decreases slowly with the increase of feed rate. The increase of hob speed and feed rate can reduce the total profile deviation, but the influence of hob speed on the total profile deviation is greater. Figure 6b is the response surface diagram of the influence of hob rotation

speed and cutting times on the total tooth profile deviation. It can be seen that the influence of hob speed and cutting times on the total tooth profile deviation is very significant; When the cutting times is small, the total deviation of tooth profile decreases with the increase of hob speed. With the increase of cutting times, the total deviation of tooth profile increases significantly, which also indicates that the increase of cutting times has a great effect on the total tooth profile deviation. When the hob speed is large, it will offset the partial influence of cutting times on the total deviation of tooth profile; Fig. 6c is the response surface diagram of the influence of feed rate and cutting times on the total profile deviation. When the cutting times is small, the total profile deviation decreases with the increase of feed rate; When the cutting times increased, the total deviation of tooth profile increased significantly, especially when the cutting times was 3, the influence on the total deviation of tooth profile was most significant.

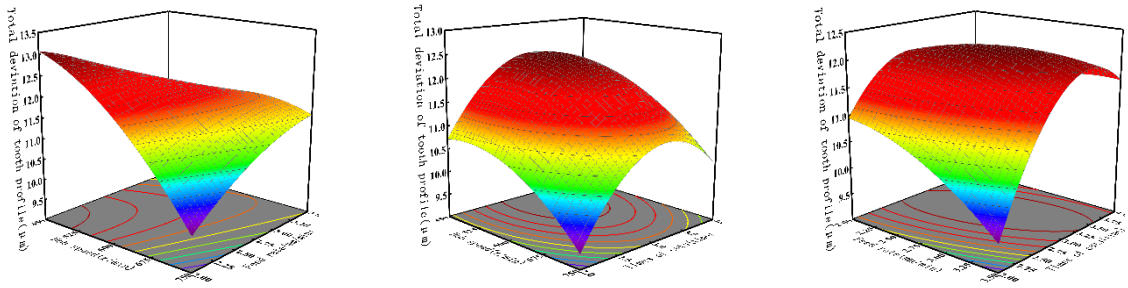

Fig. 6. Response surface diagram of total deviation of tooth profile: a) response surface influenced by V and f for F_α; b) response surface influenced by V and D_t for F_α; c) response surface influenced by f and D_t for F_α.

Figure 7 is the response surface diagram of the total helix deviation, and Fig. 7a is the response surface diagram of the combined influence of hob speed and feed rate on the total helix deviation. When the feed rate is constant, the total helix deviation decreases with the increase of hob speed. When the hob speed is constant, the total helix deviation increases slowly with the increase of feed rate. Figure 7b is the response surface diagram of the influence of hob speed and cutting times on the total helix deviation. It can be seen that the influence of hob speed and cutting times on the total helix deviation is very significant; when the cutting times is small, the total deviation of helix decreases with the increase of hob speed. When the cutting

times are large, the total helix deviation increases with the increase of hob speed, which indicates that the increase of cutting times has a great effect on the total helix deviation. Figure 7c is the response surface diagram of the influence of feed rate and cutting times on the total helix deviation. When the cutting times is small, the total helix deviation increases with the increase of feed rate; When the cutting times increased, the total helix deviation decreased significantly, especially when the cutting times was 3, the influence on the total helix deviation was most significant.

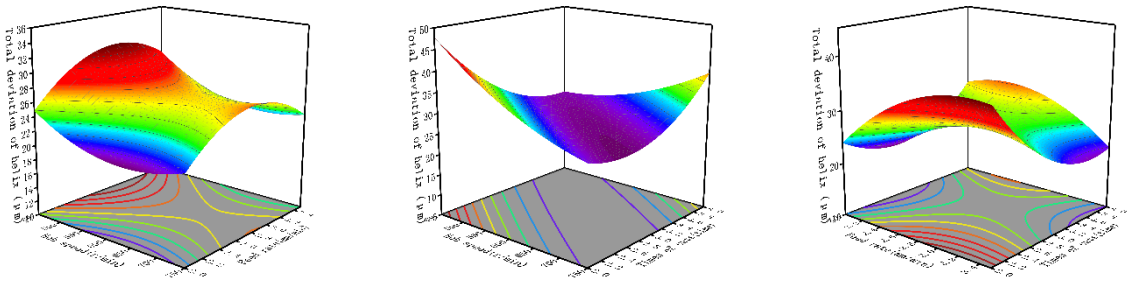

Fig. 7. Response surface diagram of total deviation of helix: a) response surface influenced by V and f for F_β; b) response surface influenced by V and D_t for F_β; c) response surface influenced by f and D_t for F_β.

Figure 8 is the response surface diagram of the cumulative total deviation of tooth spacing, and Fig. 8a is the response surface diagram of the combined influence of hob speed and feed rate on the cumulative total deviation of tooth spacing. When the feed rate is constant, the cumulative total deviation of tooth spacing increases with the increase of hob speed. When the hob speed is constant, the cumulative total deviation of tooth spacing increases rapidly with the increase of feed rate. Figure 8b is the response surface diagram of the influence of hob speed and cutting times on the cumulative total deviation of tooth spacing. When the cutting times is fixed, the cumulative total deviation of tooth spacing increases with the increase of hob speed; With the increase of cutting times, the cumulative total deviation of tooth spacing has no significant change, which indicates that the increase of cutting times has little effect on the cumulative total deviation of tooth spacing. Figure 8c is the response surface diagram of the influence of feed rate and cutting times on the cumulative total deviation of tooth spacing. When the cutting times are constant, the cumulative total deviation of tooth spacing first decreases

and then increases with the increase of feed rate; with the increase of cutting times, the cumulative total deviation of tooth spacing decreases slowly.

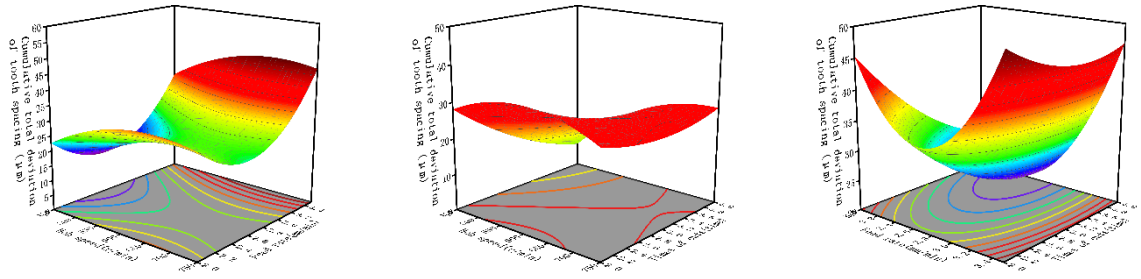

Fig. 8. Response surface diagram of cumulative total deviation of tooth spacing: a) response surface influenced by V and f for F_p; b) response surface influenced by V and D_t for F_p; c) response surface influenced by f and D_t for F_p.

Figure 9 is the response surface diagram of radial runout, and Fig. 9a is the response surface diagram of the influence of hob speed and feed rate on radial runout. When the feed rate is constant, radial runout increases with the increase of hob speed. When the hob speed is constant, the radial runout increases rapidly with the increase of feed rate. Figure 9b is the response surface diagram of the influence of hob speed and cutting times on radial runout. When the cutting times is small, radial runout first increases and then decreases with the increase of hob speed. When the times of cutting increases, the radial runout decreases slowly. Figure 9c is the response surface diagram of the influence of feed rate and cutting times on radial runout. When the cutting times is constant, radial runout first decreases and then increases with the increase of feed rate. When the times of cutting increases, the radial runout decreases slowly.

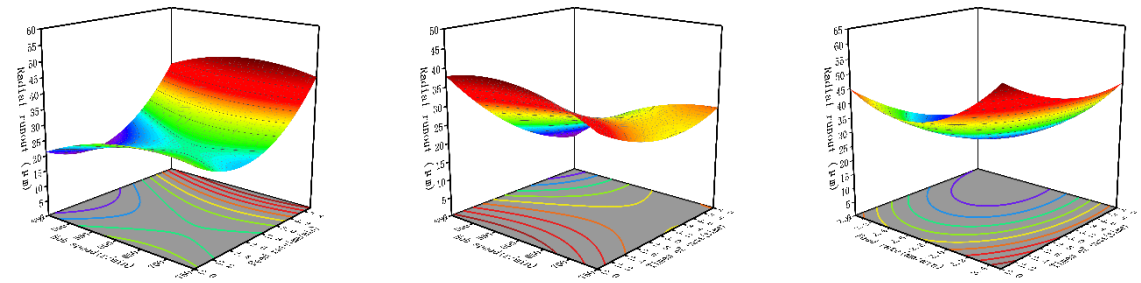

Fig. 9. Response surface diagram of radial runout: a) response surface influenced by V and f for F_r; b) response surface influenced by V and D_t for F_r; c) response surface influenced by f and D_t for F_r.

3.4. Optimization results and analysis

The optimization parameters of the NSWOA algorithm are set as follows: the initial population is 100, and the number of iterations is 500. The Pareto optimal solution set was obtained through the NSWOA algorithm optimization, and the result of the Pareto optimal solution set is shown in Fig. 10. Figure 10 shows the optimal combination of the gear hobbing process parameters distribution of all data points can satisfy the requirements of processing and geometric accuracy. It can be known through analysis that there is a significant negative correlation between the total deviation of the tooth profile and the total deviation of the helix, the cumulative total deviation of the pitch and the radial runout. The specific manifestations are as follows: With the increase of the total deviation of the tooth profile, the total deviation of the helical line, the cumulative total deviation of the pitch and the radial runout show a decreasing trend. Meanwhile, there is a significant positive correlation between the total deviation of the helical line, the cumulative total deviation of the pitch, and the radial runout. That is, as the total deviation of the helical line increases, the cumulative total deviation of the pitch and the radial runout also increase accordingly. In addition, there is also a significant positive correlation between the cumulative total deviation of pitch and radial runout.

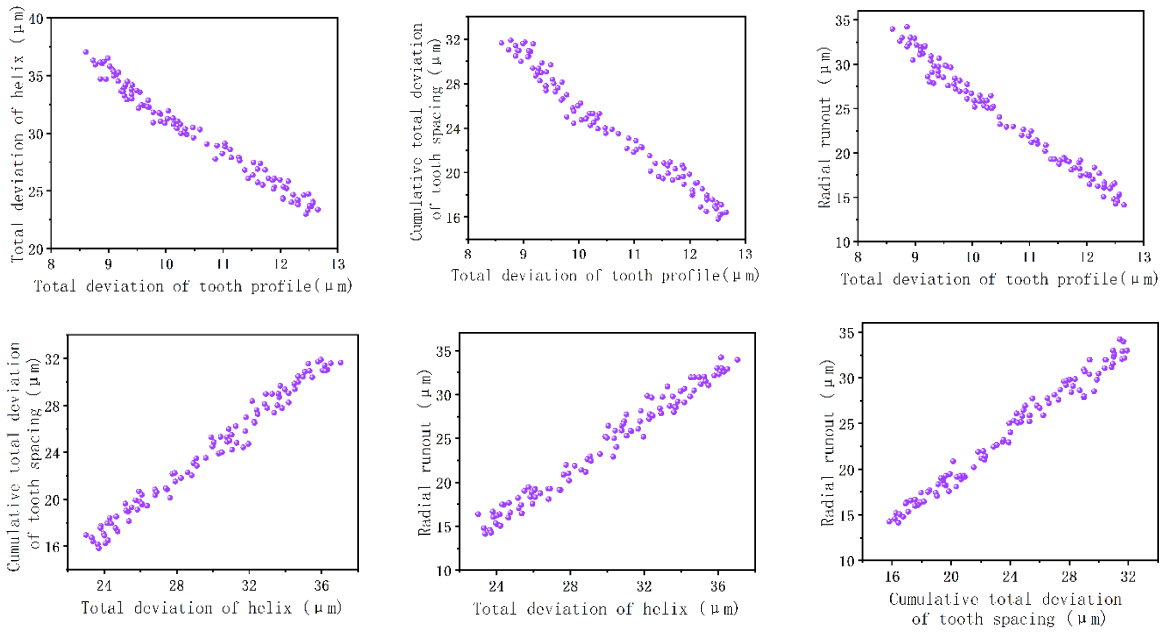

Fig. 10. Pareto optimal solution set for optimization of hobbing process parameters.

In this paper, the entropy weight-TOPSIS comprehensive evaluation method is used to conduct a systematic analysis of the Pareto solution set optimized and generated by the NSWOA algorithm. Firstly, the original data was standardized, and the weight vectors of each index were calculated using the entropy weight method as $[0.26971, 0.22237, 0.27536, 0.23256]^T$. Subsequently, through weighted standardization processing, the positive ideal solution is determined as [1, 1, 1, 1], and the negative ideal solution is determined as [0,0,0,0]. On this basis, calculate the Euclidean distances between each Pareto solution and the positive and negative ideal solutions respectively, and further obtain the comprehensive score value. The final evaluation results are shown in Table 10 as follows.

In traditional production practice, gear hobbing processing usually adopts the average value of process parameter design, specifically: the hob speed is 600 r/min, the feed rate is 2.75 mm/min, and the depth of cut is 1.125 mm. After optimization, the process parameters were adjusted to a hob speed of 750 r/min, a feed rate of 2 mm/min, and a back cut of 1.6875 mm. According to the comparative analysis of the geometric accuracy before and after optimization in Table 11, the optimization scheme has significantly improved the geometric accuracy of gear processing. Among them, the total deviation of the tooth profile has decreased by 8.04 %, the total deviation of the helix has decreased by 9.17 %, the cumulative total deviation of the pitch has decreased by 3.88%, and the radial runout has decreased by 7.45 %. The test results show that the optimized process parameters can effectively improve the geometric accuracy of gear hobbing processing, providing a solution for achieving high-precision manufacturing of gears.

Table 10. Entropy weight method – TOPSIS comprehensive evaluation.

Scheme sequence number	Positive ideal solution distance (D+)	Negative ideal distance (D–)	Composite score index	Sort
1	0.8464	0.5194	0.3803	91
2	0.4529	0.6204	0.5780	34
3	0.5315	0.4851	0.4772	58
4	0.4480	0.7106	0.6134	16

5	0.7003	0.4624	0.3977	83
...	...	...	...	...
96	0.4524	0.6313	0.5826	32
97	0.5013	0.8401	0.6263	3
98	0.6005	0.4769	0.4427	67
99	0.5001	0.5060	0.5029	48
100	0.5500	0.4794	0.4657	61

Table 11. Comparison of schemes.

	Total deviation of tooth profile [μm]	Total deviation of helix [μm]	Cumulative total deviation of tooth spacing [μm]	Radial runout [μm]
Experience scheme	12.1	26.2	21.4	25.5
The optimized scheme	11.2	24	20.6	23.6

3.5. Algorithm performance comparison

In this paper, the second-generation Non-dominated Sorting Genetic algorithm (Non-dominated Sorting Genetic Algorithms-II, NSGA-II) and the NSWOA algorithm are selected for performance comparison and analysis. The algorithm parameters are uniformly set as: population size 100 and iteration times 500. In the implementation of the NSGA-II algorithm, the interval selection strategy is adopted for chromosome screening, and the genetic operation strategy of two-point crossover and point mutation is adopted. Among them, the crossover probability is set to 0.9 and the mutation probability is set to 0.1. Figure 11 shows the distribution of the Pareto solution set obtained from a single run of the NSGA-II algorithm.

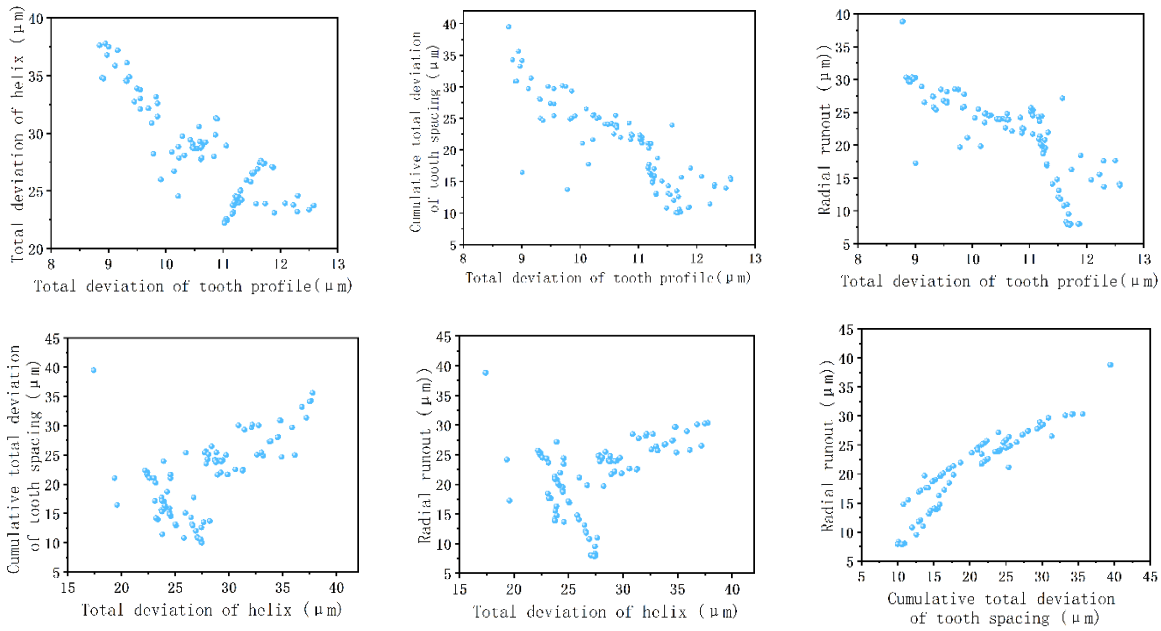

Fig. 11. Non-dominated solution diagram of NSGA-II algorithm.

Through multiple independent tests of the two algorithms, Table 12 statistically presents the performance comparison data of 10 runs each for NSGA-II and NSWOA. It can be seen from the data analysis in Table 12 that NSGA-II has obvious advantages in computing efficiency, and its running time is less than 50 % of that of NSWOA. However, NSWOA performs more prominently in the optimization performance of the objective function. Both its optimal solution quality and average solution quality are superior to NSGA-II, demonstrating a stronger global search ability. Comprehensive comparison shows that in the current application scenarios, NSWOA shows higher applicability compared with NSGA-II and can approach the optimal solution of the problem more effectively.

Table 12. Comparison of algorithm performance and running time.

Algorithm	Parameter	Total deviation of tooth profile [μm]	Total deviation of helix [μm]	Cumulative total deviation of tooth spacing [μm]	Radial runout [μm]	Running time [s]
NSGA-II	Optimal value	8.5	17.25	9.98	8.2	2.8

	Mean value	12.36	26	10.33	23	3.2
NSWOA	Optimal value	8.45	17	8	7.63	9.39
	Mean value	10.43	24.5	9.5	20.6	9.48

4. Conclusions

In this paper, the response surface method is used to study the process of gear hobbing. The results of hobbing experiment, model building and optimization analysis show that:

1. based on the response surface test data, the regression models of total profile deviation, total helix deviation, cumulative total deviation of tooth spacing and radial runout were established, and the reliability of the models was tested by variance analysis;
2. the interaction of different process parameters on total profile deviation, total helix deviation, cumulative total deviation of tooth spacing and radial runout was analyzed by using response surface diagram. The interaction effects of hob speed, feed rate and cutting times on total profile deviation, total helix deviation, cumulative total deviation of tooth spacing and radial runout are significant. The rotational speed of the hob has the greatest influence on the geometric accuracy, followed by the feed rate. The cutting times have a relatively large influence on the total deviation of the tooth profile and the total deviation of the helix, but have a relatively small influence on the cumulative total deviation of the tooth spacing and the radial runout;
3. the objective functions of total profile deviation, total helix deviation, cumulative total deviation of tooth spacing and radial runout were established respectively. With hob speed, feed rate and cutting times as optimization variables, the total profile deviation, total helix deviation, cumulative total deviation of tooth spacing and radial runout as optimization objectives, the established model was solved by using NSWOA algorithm. The Pareto solution set within the constraint range is obtained, and the optimal scheme optimized by NSWOA algorithm is determined by combining entropy weight method and TOPSIS

method. Compared with the empirical scheme, the total profile deviation is reduced by 8.04%, the total helix deviation is reduced by 9.17 %, the cumulative total deviation of tooth spacing is reduced by 3.88 %, and the radial runout is reduced by 7.45 % after optimization.

Fundings

The research is supported by the Natural Science Foundation of Gansu Province (25JRRA092) and College Teachers Innovation Fund of Gansu Province (2025A-029).

Conflict of interests

The Authors declare that there are no known competing financial interests or personal relationships that could influence the work reported in this paper.

REFERENCES

1. Chen Y, Liu X, Yan X et al. Investigation on geometrical morphology of tooth surface finished by green high-speed dry hobbing for gear precision machining. *International Journal of Precision Engineering and Manufacturing-Green Technology*, **10**: 1141–1154, 2023, doi:10.1007/s40684-022-00459-3.
2. Sun S L, Wang S L, Wang Y W, etal. Prediction and optimization of hobbing gear geom etric deviations. *Mechanism and Machine Theory*, **120**: 288-301, 2018, doi:10.1016/j.mech machtheory.2017.09.002.
3. Hu Q S, Li H. Research on hobbing accuracy of flexspline tooth profile of harmonic drive. *Journal of Advanced Mechanical Design Systems and Manufacturing*, **18**(2), 2024, doi:10.1299/jamdsm.2024jamdsm0008.
4. Wang J, Wang J, Dong J P. Prediction and optimization of hobbing parameters for minimizing energy consumption and gear geometric deviations. *Advances in Mechanical Engineering*, **16**(4):1-16, 2024, doi:10.1177/16878132241236374.
5. Matsuo K, Suzuki Y, Fujiki K. Analysis of the effect on gear accuracy of workpiece/tool positioning

accuracy in the hobbing process. *Journal of Advanced Mechanical Design Systems and Manufacturing*, **11**(6), 2017, doi:10.1299/jamdsm.2017jamdsm0071.

6. Zhou J L, Sun Z H, Tan Q, et al. Dry gear hobbing machining experiment and research on process parameters. *Applied Mechanics and Materials*, **538**: 95-99, 2014, doi:10.4028/www.scientific.net/AMM.538.95.
7. Dong X, Liao C, Shin Y C, et al. Machinability improvement of gear hobbing viaprocess simulation and tool wear predictions. *The International Journal of Advanced Manufacturing Technology*, **86**(9):2771–2779, 2016, doi:10.1007/s00170-016-8400-3.
8. Klockea F, Brechera C, Löpenhausa C, et al. Calculating the workpiece quality using a hobbing simulation. *Procedia CIRP*, **41**:687-691, 2016, doi:10.1016/j.procir.2015.12.045.
9. Huai W B, Shi Y Y, Du Y Y, et al. Optimization of milling process parameters for multi-objective superalloy GH4169. *Modern Manufacturing Engineering*, (11): 1-6+12, 2020, doi:10.16731/j.cnki.1671-3133.2020.11.001.
10. Kane M M, Ivanov B V, Zagorskaya N B. Optimizing the hobbing of cylindrical gears. *Russian Engineering Research*, **34**(8): 526-529, 2014, doi:10.3103/S1068798X14080061.
11. Li X, Yang Y, Zou Z, et al. Study on the effect of force-thermal coupling error on the gear hobbing accuracy and its visualization. *The International Journal of Advanced Manufacturing Technology*, **102**: 583–594, 2019, doi:10.1007/s00170-018-3186-0.
12. Sant'Anna D R, Mundim R B, Borille A V, et al. Experimental approach for analysis of vibration sources in a gear hobbing machining process. *Journal of the Brazilian Society of Mechanical Sciences and Engineering*, **38**: 789-797, 2016. doi:10.1007/s40430-014-0300-6.
13. Anupam B, Can B K, Seyedali M. Advances in swarm intelligence: variations and adaptations for optimization problems. *Studies in Computational Intelligence*, **1054**, 2023.
14. Wu X Q, Zhang C Y. Optimization algorithm of hobbing cutting parameters based on particle swarm optimization SVR. *In 2018 International Conference on Computational Science and Engineering*, Qingdao, 23-28, 2018.
15. Wang Y. Z., Xu H. K., Shen H., et al. A study on the effect of gear hobbing process parameters on the residual stress of the tooth root. *Applied Sciences*, **14**(597), 2024, doi:10.3390/app14020597.

16. Yuan B, Han J, Wu L L, et al. Comprehensive contour error prediction model and experi mental study of hobbing tooth surface based on particle swarm optimization.*China Mecha nical Engineering*, **27**(20): 2705-2711, 2016, doi:10.3969/j.issn.1004-132X.2016.20.002.
17. ISO 1328-1, Cylindrical gears - ISO system of flank tolerance classification - Part1: Definitions and allowable values of deviations relevant to flanks of gear teeth, *International Standard*, 2013.
18. Sanjeevi R, Arun K G, Radha K B. Optimization of machining parameters in plane surface grinding process by response surface methodology, *Materials Today: Proceedings*, **37**(2): 85-87, 2021. doi:10.1016/j.matpr.2020.04.075.
19. Wang Y, Wang G, Fan Y Z, et al. A virtual measurement method for evaluating the gear radial composite deviation based on point cloud data. *Results in Engineering*, **22**, 2024, doi:10.1016/j.rineng.2024.102380.
20. Kharka V, Jain N K, Gupta K. Influence of MQL and hobbing parameters on microgeometry deviations and flank roughness of spur gears manufactured by MQL assisted hobbing. *Journal of Materials Research and Technology*, **9**(5): 9646-9656, 2020, doi:10.1016/j.jmrt.2020.06.085.
21. Jangir P, Jangir N. Non-dominated sorting whale optimization algorithm (NSWOA): A multi-objective optimization algorithm for solving engineering design problems. *Global Journal of Researches in Engineering: F Electrical and Electronics Engineering*, **17**(4), 2017, doi:10.19080/ETOAJ.2018.02.555579.
22. Seyedali M, Jin S D, Andrew L. Nature-inspired optimizers theories, literature reviews and applications. *Studies in Computational Intelligence*, **811**, 2020, doi:10.1007/978-3-030-12127-3.